ELECTRONIC STRUCTURE AND PARITY EFFECTS IN CORRELATED NANOSYSTEMS

Adam Rycerz[*1] and **Jozef Spałek**[1]

[1] Marian Smoluchowski Institute of Physics, Jagiellonian University, Reymonta 4, 30–059 Kraków, Poland

Key words Correlated nanosystems, parity effects, EDABI method
PACS 71.27.+a, 73.63.-b

We discuss the spectral, transport and magnetic properties of quantum nanowires composed of $N \leqslant 13$ atoms and containing either even or odd numbers of valence electrons. In our approach we combine **E**xact **D**iagonalization and **Ab I**nitio calculations (EDABI method). The analysis is performed as a function of the interatomic distance. The momentum distribution differs drastically for those obtained for even N with those for odd N, whereas the Drude weight evolve smoothly. A role of boundary conditions is stressed.

For low–dimensional systems, the procedure starting from the single–particle picture (band structure) and including subsequently the interaction via a *local* potential may not be appropriate. In this situation, one resorts to parametrized models of correlated electrons, where the single–particle and the interaction-induced aspects of the electronic states are treated on equal footing. The single–particle wave–functions are contained in the formal expressions for model parameters and should be calculated separately. We have proposed [1] to combine the two efforts in an exact manner.

A separate question concerns the role of boundary conditions (BC*s*) in atomic rings, particularly under the presence of spin frustration for *odd* number of atoms. This problem was investigated numerically [2] and the optimal BC*s* for a correlated system were found to remain usually the same as for the ideal Fermi gas on the lattice. However, the general proof of this basic fact have been elaborated very recently [3].

In our method of approach (EDABI), we determine ***first*** rigorously the energy of interacting particles in terms of the microscopic parameters for a given BC*s* and then allow the single–particle wave functions (contained in the parameters) to relax in the correlated state. The method has been overviewed in [4], so we concentrate here on its application to nanochains of $N \leqslant 13$ atoms, containing either *even* or *odd* number of electrons. The discussion of parity effects complements our recent study of correlated nanochains [5], where we consider the properties of even–N systems only.

We consider the system of N lattice sites, each containing a single valence orbital and (i.e. hydrogenic–like atoms). Including *all* long–range Coulomb interaction and neglecting other terms, one can write down the system Hamiltonian in the form

$$H = \epsilon_a^{\rm eff} \sum_j n_j + t \sum_{j\sigma} \left(e^{-i\phi/N} c_{j\sigma}^{\dagger} c_{j+1\sigma} + \text{h.c.} \right) + U \sum_i n_{i\uparrow} n_{i\downarrow} + \sum_{i<j} K_{ij} \delta n_i \delta n_j, \qquad (1)$$

where $\delta n_i \equiv n_i - 1$, $\epsilon_a^{\rm eff} = \epsilon_a + N^{-1} \sum_{i<j} (2/R_{ij} + K_{ij})$ (in Ry) is the effective atomic level, R_{ij} is the distance between the i–th and j–th atoms, t is the nearest–neighbor hopping, ϕ is the fictitious (dimensionless) flux through the ring, U and K_{ij} are the intra– and inter–site Coulomb repulsions. The last term represents the *correlated* part of the long–range interaction. One can easily show, that the unitary transformation $c_{j\sigma} \rightarrow e^{-i\phi j/N} c_{j\sigma}$ allows to accumulate all the complex phase factors in the terminal

* Corresponding author, e-mail: adamr@th.if.uj.edu.pl
Present address: Instituut–Lorentz, Universiteit Leiden, P.O. Box 9506, NL–2300 RA Leiden, The Netherlands

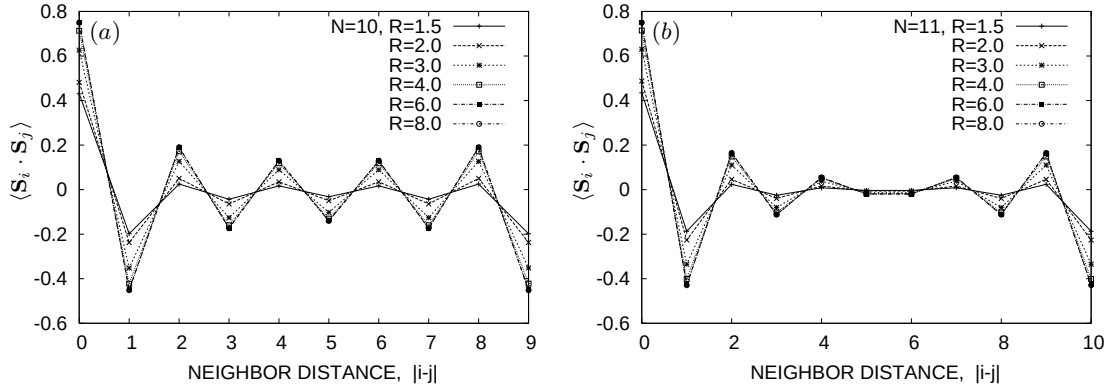

Fig. 1 Parity effect on spin ordering: spin–spin correlations for nanochains of $N = 10$ (a) and $N = 11$ (b) atoms. The values of the interatomic distance R are specified in the atomic units ($a_0 = 0.529$ Å).

hopping term [6], which than takes the form $t(e^{-i\phi}c^{\dagger}_{1\sigma}c_{N\sigma} + \text{h.c.})$ and can be regarded as *generalized* BC Such form is particularly convenient for numerical purposes, since majority of the hopping terms are real. Hereinafter, we do not distinguish between the system with a fictitious flux and with generalized BC*s*.

The Hamiltonian (1) is diagonalized in the Fock space with the help of Davidson technique [7]. As the microscopic parameters ϵ_a^{eff}, t, U, and K_{ij} are calculated in the Gaussian basis composing the Wannier functions, the orbital size of the $1s$–like state is subsequently adjusted to obtain the minimal ground state energy E_G as a function of the interatomic distance R.

We now discuss the spin–spin correlations $\langle \mathbf{S}_i \cdot \mathbf{S}_j \rangle$ in the system ground state as a function of the discrete neighbor distance $|i-j|$ and R, as presented in Fig. 1. The effect of spin frustration in the half–filled case ($N_e = N$) is remarkable for large R, where the quasi–long range order for $N = 10$ (*cf.* Fig. 1a), indicating the power–law decay of $\langle \mathbf{S}_i \cdot \mathbf{S}_j \rangle$ for the Heisenberg spin chain, disappears for $N = 11$ (*cf.* Fig. 1b), where we observe a fast, exponential decay. For small values of R, however, the effect is weaker, since the antiferomagnetic order is reduced by charge fluctuations [5]. We also observe, that the values of the spin gap (not shown) are significantly higher for odd N in the large–R range, what can be explained by the fact, that the ground–state energy of the Heisenberg antiferromagnet is of the order $E_G \sim JS(S+1)$, where $J = 4t^2/(U-K)$ is the kinetic–exchange coupling parameter and S is the total spin value. One can expect now, that the following inequality is satisfied $E_G^{S=\frac{3}{2}} - E_G^{S=\frac{1}{2}} > E_G^{S=1} - E_G^{S=0}$, where the left– and the right–hand sides represent the spin gap for the *odd*– and the *even*–N systems, respectively (both at the minimal–spin configuration). The detailed behavior of the system spin, as well as the charge and the optical gaps will be discussed elsewhere. In the remaining part of this paper we focus on the parity effect for the Fermi–Dirac distribution function and the transport properties.

The electron momentum distribution for nanochains with *optimal* BC*s* is shown in Fig. 2a. The discrete momenta, corresponding to the solutions of the single–particle part of the Hamiltonian (1) for a finite N, are given by

$$k_q(\phi) = \frac{2\pi q - \phi}{N}, \quad 0 \leqslant q < N. \tag{2}$$

The *optimal* BC*s*, corresponding to the minimal ground–state energy E_G, are realized for $\phi = 0$ when $N = 4n + 2$ (*periodic* BC), $\phi = \pi$ when $N = 4n$ (*antiperiodic* BC) and $\phi = \pi/2, 3\pi/2$ when N is odd [3]. A basic analysis of Eq. (2) shows, that for the optimal BC*s*, the Fermi momentum state $k_F = \pi/2R$ is newer reached for even N, whereas for odd N it happens, for a single value of q. This circumstance has tremendous implications for electronic structure of a nanochain, however, of almost does not effect its transport properties, as we show in the end part of this paper.

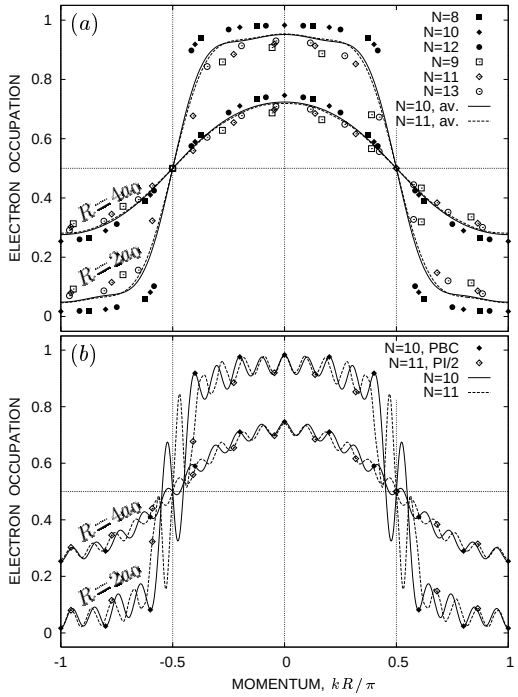

Fig. 2 Electron momentum distribution for chains of $N = 8 \div 13$ atoms: (a) datapoints for *optimal* boundary conditions (BC*s*) and the sample $n(k)$ curves averaged over BC*s* (*solid* lines); (b) the original $n(k_q(\phi))$ functions used for the averaging.

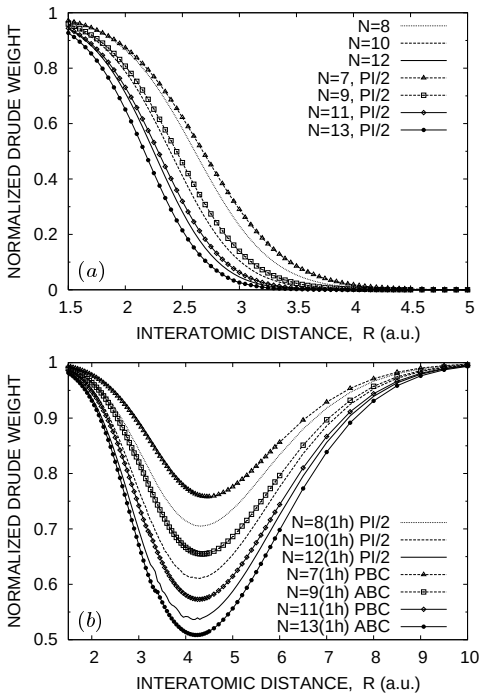

Fig. 3 Normalized Drude weight for nanochains in the *half–filled* case (a), and for a system with a single hole (b). The *optimal* boundary conditions are specified for each curve.

The remarkable feature of these results, is that the datapoints for different but even N (*cf.* full symbols in Fig. 2a) locate smoothly on the universal curve (for each R), when optimal BC*s* are applied. This is not the case for odd N (*cf.* open symbols in Fig. 2a), when the systematic dependence on N suggests quite slow convergence to the even–N results with the increasing N. However, the discussion of $N \to \infty$ limit is beyond the scope of this paper, since we concentrate here on nanochains. To analyze such systems in detail, we have displayed in Fig. 2b the continuous electron momentum distribution obtained for the dense set of $k_q(\phi)$ defined by Eq. (2), when $\phi \in \langle 0, 2\pi)$. The datapoints corresponding to optimal BC for $N = 10$ and 11 are also presented to show, they are situated close to the different local extrema of $n(k_q(\phi))$ (e.g. maxima for even N and minima for odd, or *vice versa*). Except of different frequency of internal oscillations (equal to $2NR$), the $n(k_q(\phi))$ functions for $N = 10$ and 11 looks almost identically. This is the reason, why various physical properties of small clusters are often averaged over BC, particularly in 2D [6]. We also perform such averaging to obtain almost size–independent $n(k)$ functions, drawn again in Fig. 2a (the details of the averaging procedure will be published elsewhere). However, the elimination of the internal oscillations for a given N may only be considered as an approximation of $N \to \infty$ scaling procedure, and in the case of momentum distribution $n(k)$ seems less accurate then fitting the Luttinger–liquid formulas to even N data, which we proposed before [5]. Nevertheless, the common nature of either original $n(k_q(\phi))$ or averaged $n(k)$ functions for both even and odd N, illustrated in Fig. 2, helps to understand why the chain parity does not effect its Drude weight even for optimal boundary conditions, when the structure of the momentum space is significantly different.

The *normalized* Drude weight, shown in Fig. 3, is defined in the standard manner [8]

$$D = -\frac{1}{\langle T \rangle} \left. \frac{\partial^2 E_G}{\partial \phi^2} \right|_{\phi=\phi_{\min}}, \tag{3}$$

where $\langle T \rangle$ is the average kinetic energy and $\phi_{\min}$ denotes optimal BC*s*. In the half–filled case $N_e = N$ (*cf.* Fig. 3a) Drude weight gradually decrease with N, as we have shown for even N [5]. The most interesting feature of these results is, that the curves for odd N fits smoothly between those for even N, with very weak parity effect (totally incomparable with that present in the charge gap and electron momentum distribution, when optimal BC are applied). This observation can be understood when we take into account, that the Drude weight defined by Eq. 3 is the *integral* quantity, involving the summation over all the excited states of the Hamiltonian Eq. (1), so it cannot be determined only by the electronic structure near the Fermi points, particularly for a small system.

The parity effect on Drude weight disappears for the system with a single hole ($N_e = N - 1$, *cf.* Fig. 3b), in which the magnetic frustration is absent. For this case, the Drude weight evolution with R is very interesting. In the weak–correlation range ($R/a_0 \lesssim 2$) the chain shows a highly–conducting behavior for each N. Next, in the intermediate range ($R/a_0 = 4 \div 5$) the Drude weight decrease rapidly with N, indicating an insulating (Mott–Hubbard) state in the large–N limit. In the strongly–correlated range ($R/a_0 \sim 10$) the Drude weight approaches again its maximal value $D = 1$. Such a behavior can be explained, when we analyze the situation in two steps: *First*, for low values of R, the bandwidth–to–interaction ratio is small, and the system with a single hole does not differ significantly from a half–filled one. This is why in both cases Drude weight decreases gradually with both N and R, as the tunneling amplitude through the barrier of a finite width. *Second*, for the largest values of R, the system can be described by an effective $t - J$ model [9] with a coupling constant $J = 4t^2/(U - K) \ll |t|$ (where $K \equiv K_{j,j+1}$ denotes the nearest neighbor Coulomb repulsion), which corresponds to an asymptotically–free hole motion. Then, it become clear that in the intermediate range the Drude weight has to suppressed, what can be interpreted in terms of a partially localized spin–ordered state. It would be very interesting to test experimentally this result, possibly for a mesoscopic atomic ring.

In summary, we have shown that a nanochain parity effect strongly its electronic structure and momentum distribution, and that the effects are opposite for these two principal characteristics. Namely, the presence of a discrete momenta in the Fermi point reduce significantly the finite–size effects on the system charge–gap, but amplifies them in the case of momentum distribution. On the other hand, the parity effect is weak, or even absent in the case if system transport properties. Additionally, an interesting crossover behavior has been identified for the chain with a single hole, for which the quantum–liquid regions are separated by a partly localized state.

The support from the Polish Science Foundation (FNP) is acknowledged.

References

[1] J. Spałek, *et al.*, *Phys. Rev. B* **61**, 15676 (2000); A. Rycerz, J. Spałek, *ibid.* **63**, 073101 (2001); **65**, 035110 (2002).
[2] R. Jullien, R. M. Martin, *Phys. Rev. B* **26**, 6173 (1982); B. Fourcade, G. Sproken, *ibid.* **29**, 5096 (1984); R. M. Fye, *et al.*, *ibid.* **44**, 6909 (1991); K. Rościszewski, A. M. Oleś, *J. Phys. Cond. Mat.* **5**, 7289, (1993).
[3] E. H. Lieb, *Phys. Rev. Lett.* **73**, 2158 (1994); F. Nakano, *J. Phys. A* **33**, 5429 (2000); *ibid.* **37**, 3979 (2004).
[4] J. Spałek, *et al.*, *Acta Phys. Polon. B* **31**, 2879 (2000); *ibid.* **32**, 3189 (2001); in *Concepts in Electron Correlation*, Proc. of the NATO Adv. Res. Workshop, eds A.C. Hewson and V. Zlatić, pp. 257–268, Kluwer, Dordrecht (2003).
[5] A. Rycerz, J. Spałek, *Eur. Phys. J. B* **40**, 153 (2004).
[6] D. Poilblanc, *Phys. Rev. B* **44**, 9562 (1991).
[7] E. R. Davidson, *J. Comput. Phys.* **17**, 87 (1975).
[8] B.S. Shastry and B. Sutherland *Phys. Rev. Lett.* **65**, 243 (1990); J.A. Millis and S.N. Coppersmith, *Phys. Rev. B* **42**, 10807 (1990); D. Góra, K. Rościszewski, A.M. Oleś, J. Phys. Condensed Matter **10**, 4755 (1998).
[9] P. W. Anderson, *Phys. Rev.* **115**, 2 (1959); W. F. Brinkman and T. M. Rice, *Phys. Rev. B* **2**, 1324 (1970); K. A. Chao, J. Spałek, and A. M. Oleś, *J. Phys. C* **10**, L271 (1977).